# Physics of attosecond pulses produced via high harmonic generation

Varju, Katalin; Johnsson, Per; Mauritsson, Johan; L'Huillier, Anne; Lopez-Martens, Rodrigo

*Published in:*
American Journal of Physics

*DOI:*
10.1119/1.3086028

2009

# Physics of Attosecond Pulses Produced via High Harmonic Generation

K. Varjú,[1] P. Johnsson,[2] J. Mauritsson,[2] R. López-Martens,[3] and A. L'Huillier[2]

[1]*Department of Optics and Quantum Electronics, University of Szeged, Hungary*
[2]*Department of Physics, Lund University, P. O. Box 118, SE-221 00 Lund, Sweden*
[3]*Laboratoire d'Optique Appliquée, Ecole Nationale Supérieure des Techniques Avancées (ENSTA) - Ecole Polytechnique CNRS UMR 7639, 91761 Palaiseau Cedex, France*

(Dated: November 18, 2008)

The physics of extreme ultraviolet attosecond pulse trains generated during the interaction between an intense laser pulse and a gas medium is presented, including a simple modeling based on the solution of classical equations of motion for an electron in an oscillating laser field. The reconstruction of attosecond beating by interference of two-photon transition (RABITT) technique is described and used to determine the pulse duration of the emitted attosecond pulses. This work forms the basis of a laboratory practical of an Advanced Atomic Physics course taught at Lund University for MSc students in Physics and Engineering Physics.

PACS numbers:

## INTRODUCTION

Atoms in molecules move on the femtosecond ($10^{-15}$ s) timescale, whereas the much lighter electrons, responsible for interatomic forces, change distribution on the attosecond ($10^{-18}$ s) timescale. Using attosecond pulses as probes enables one to capture the temporal evolution of electronic processes such as relaxation in case of an inner-shell vacancy [1]. A fundamental limit of the achievable pulse duration for a light source is given by the period of the carrier component of the radiation. Lasers operating in the visible and infrared spectral region are limited to pulse durations of a few femtosecond. To reach the attosecond regime, the coherent radiation has to be extended to shorter wavelengths.

Almost twenty years ago, high-order harmonic generation (HHG) in gases [2] , which provides a large spectral bandwidth in the extreme ultraviolet (XUV) range, was proposed as a possible candidate for the production of attosecond pulse trains (APTs) [3, 4]. It took seventeen years for scientists to be able to demonstrate these APTs experimentally, and almost at the same time to produce isolated attosecond pulses [5, 6]. Over the last couple of years, the metrology and applications of attosecond pulses have progressed rapidly [5–8], and *attophysics* has become a "hot" field of research [9, 10].

Alternative methods to produce attosecond pulses include harmonics from plasma surfaces [11] and stimulated Raman scattering [12]. Here we restrict the discussion to the method of gas harmonic generation.

In this article we describe the process of HHG, using a simple model, and the characterization of attosecond pulse trains. This forms the basis of a laboratory practical that has been taught over the last four years at Lund University (LU) for MSc students reading a course in Advanced Atomic Physics. We believe that it is an advantage for students to be in contact with a hot topic - producing numerous articles in high impact journals each year. The laboratory practical performed at LU is based on the experimental setup used for our research. We hope that even those - who do not have access to amplified femtosecond laser pulses will find this article useful - and appreciate the interesting physics. Our laboratory practical includes

- modelling the HHG process, using classical calculations
- generating high-order harmonics by focusing the femtosecond laser pulse to a gas target,
- recording a so-called RABITT-scan using an optical cross correlation setup and
- analyzing the scan, thus obtaining information on the attosecond pulse's temporal structure.

To prepare the laboratory practical, the students have to solve a few exercises, some of them requiring (simple) numerical calculations. The intention of these exercises is to provide a good understanding of the underlying physics of HHG. It should be possible to solve them using the information provided in this paper.

## HIGH-ORDER HARMONICS

### Non-linear process

During normal light propagation, the light's electric field introduces a polarization in the material, redistributing the charges within the medium. In this way the charges in the material are made to oscillate with the same frequency as the electric field, re-emitting radiation at the same wavelength as the incoming field. In this linear model it is assumed that the charges in the material are free to follow the electric field, describing a perfect sinusoidal oscillation. However, in a real system, there

exists higher-order frequency terms in the induced polarization. This means that when a light field propagates through a material, the introduced polarization of the medium also gives rise to radiation with frequencies that are multiples of the incident frequency. Normally, the efficiency of such process is small and rapidly decreases with the order of the process. [13]

To achieve high laser intensities, where nonlinear effects play a noticeable role, ultrashort (femtosecond) laser pulses are used. In this case, energy can be concentrated to a very short time interval, resulting in optical pulses with modest energies but high peak powers. As an example, a 50 fs laser pulse with an energy of 1 mJ exhibits a peak power of 20 GW. If this pulse is focused to a $(100\ \mu\text{m})^2$ spot, the peak intensity will be 0.2 PW/cm$^2$, corresponding to an electric field strength of around 0.4 GV/cm. For comparison, an intra-atomic field strength is typically of the order of 1 GV/cm. The electric fields associated with ultrashort pulses are thus comparable to the fields binding the electron to the atom, indicating that extreme non-linear processes are likely to occur.

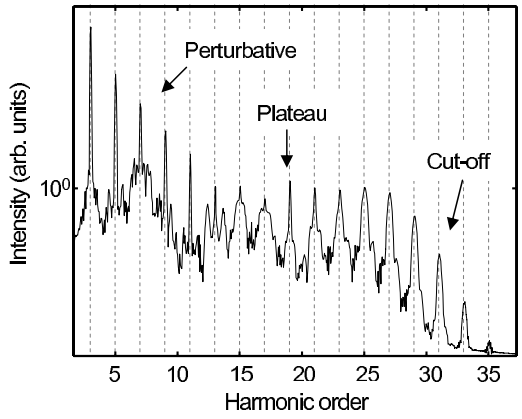


FIG. 1: A simulated harmonic spectrum generated in argon using a laser pulse of peak intensity $1.4 \cdot 10^{14}$ W/cm$^2$.

When a laser pulse is focused to a high intensity in a gas, high-order harmonics of the driving field are generated, propagating collinearly with the laser field. Only odd multiples of the driving frequency can be seen and for a typical harmonic spectrum (see Fig. 1) the intensity drops rapidly accross the first few harmonics. This is what one would expect from a perturbative approach where the efficiency of the process rapidly decreases with order. What cannot be explained with this approach is the far-reaching plateau, in which the harmonics have almost constant intensity, ending in an abrupt cut-off. High-order harmonics were first seen in 1988 [2] and the harmonic plateau may extend up to very high orders (above the 200th)[14].

**Experimental setup & technique**

A picture of the experimental setup can be seen in Fig. 2. The laser used in this laboratory exercise is a Ti:Sapphire-based laser system using Chirped Pulse Amplification (CPA), delivering pulses with 2 mJ energy and 40 fs duration at 800 nm central wavelength. After reflection losses, and the beam splitter, we use about 1 mJ to generate harmonics, which corresponds to a peak power of 25 GW. The 8 mm Gaussian laser beam is focused using a 1 m spherical focusing mirror to provide a generating intensity of $2 \times 10^{14}$W/cm$^2$. We can also determine the electric field amplitude ($E$) from

$$I = \frac{1}{2}\varepsilon_0 c\,|E|^2 \tag{1}$$

where $\varepsilon_0$ is the permittivity of free space and $c$ the speed of light in vacuum. The amplitude of the electric field in this case is $E_0$ =0.4 GV/cm, which is indeed comparable to the atomic field strength.

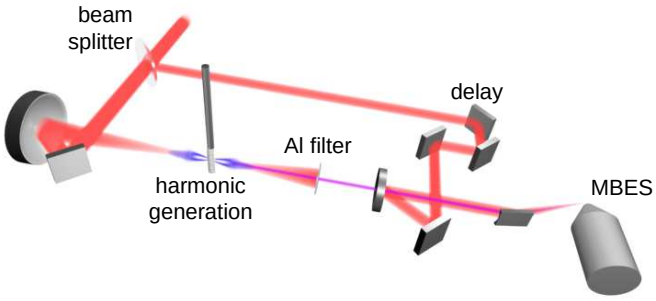


FIG. 2: Experimental setup: the laser beam is divided to a pump and a probe lines. The pump generates the high-order harmonics, that are filtered by an aluminum filter, and then recombined with the delayed probe using a holed diverging mirror. The two beams are refocused to the sensitive region of the MBES.

**The three-step model**

To explain the process of high-order harmonic generation one has to consider the fact that the strength of the electric field of the laser is comparable to that of the atomic potential - implying that consequently the electron cannot be assumed to be in a bound state during its interaction with the laser field. A commonly-used description of HHG is the three-step semi-classical model introduced in 1993 [15, 16]. This model assumes an atomic potential - strongly distorted by the electric field of the laser - as illustrated in Fig. 3. There is a finite chance for the electron to tunnel through the potential barrier, and to propagate in the laser field free from the ionic potential. The laser field accelerates the electron away - and a quarter of a period later - when the electric

field changes sign, the electron is driven back towards the ionic core, where it might recombine.

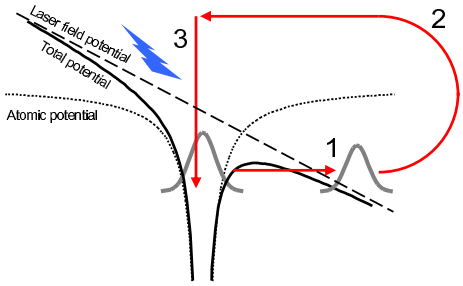


FIG. 3: The three-step model of harmonic generation. When the external electric field is near its maximum, the total potential of the atom (dotted line) and the laser field (dashed line) forms a barrier (solid line) through which the electron may ionize by tunneling (1). When in the continuum, the electron is accelerated by the oscillating electric field, gaining kinetic energy (2). Finally, when the field changes sign, the electron may be accelerated back to the vicinity of the ion core where it recombines, and a photon is emitted (3).

If the electron recombines, its kinetic energy gained from the acceleration in the field, depends on the time of tunneling and the time of recombination, and determines the energy of the emitted high energy photon. The maximum kinetic energy the electron can gain from the laser field is approximatelly $3.2U_P$, where $U_P$ is the ponderomotive energy, that depends on the field intensity and frequency. This result can be verified by the classical model, as described in the next section. The ponderomotive energy corresponds to the average kinetic energy of a free electron in an electric field, and is given by

$$U_P = \frac{e^2 E_0^2}{4m\omega^2} \tag{2}$$

where $e$ is the electron charge, $E_0$ is the amplitude of the electric field, $\omega$ is the laser angular frequency and $m$ is the electron mass. The total maximum photon energy, or *cut-off* energy, is then $I_P + 3.2U_P$, where $I_P$ is the ionization potential of the atom. In our experimental conditions, we obtain a ponderomotive energy $U_P$=11.9 eV. The harmonics are generated in a gas cell (HHG), filled with Argon to a static pressure of around 15 mbar. Ar has an ionization potential of 15.8 eV, which leads to a harmonic cutoff order equal to 33. This is verified in the experiment.

All possible photon energies up to the maximum energy are obtained with approximately equal probability, leading to the long plateau of peaks of almost equal amplitude. The reason we get discrete peaks at the harmonic frequencies and not a continuous spectrum is because the process is periodic in time: the electron may tunnel out each time when the electric field is close to maximum. Since the gas is isotropic there is no difference in the case the electron tunnels out when the electric field is $-E_0$ or $+E_0$. The period of the process is therefore $T/2$ where $T$ is the laser period. This leads to the periodicity of $2\omega$ in the frequency domain - and we only observe odd harmonics [17].

### Classical model

When the electron recombines with its parent ion, a short burst of light is emitted. The properties of the emitted pulse are directly linked to those of the recombining electron, making the temporal profile of the emitted light crucially dependent on the electron dynamics in the continuum.

Performing classical calculations provide an intuitive picture of the process. We consider what happens to a single electron accelerated along a certain trajectory by the electric field of the laser, and illustrate it in Fig. 4, as explained in Exercise I. This simple picture allows us

- to determine the position of the cut-off corresponding to the electron returning with the maximum energy,
- to identify several trajectories contributing to HHG (called the short and the long, as illustrated in the figure) and
- to predict the temporal characteristics of the emitted light, and in particular its chirp, i.e. its frequency modulation in time.

### Exercises I

*Electron motion in a laser field*

The atom is exposed to a laser field $E(t) = E_0 \sin(\omega t)$ where $E_0$ is the field amplitude and $\omega$ the laser frequency. An electron tunnels through the Coulomb barrier and is released into the continuum with zero velocity at time $t = t_i$. We neglect the influence of the atomic potential and assume that the only force experienced by the electron is that from the electric field : $F(t) = -eE(t)$, where $e$ is the elementary charge. The position of the electron as a function of time $t \geq t_i$ is given by

$$x(t) = \frac{eE_0}{m\omega^2}\left[\sin(\omega t) - \sin(\omega t_i) - \omega(t - t_i)\cos(\omega t_i)\right] \tag{3}$$

*Return of the electron*

With the help of the above equation it is possible to find the tunneling times ($t_i$) for which the electron may return to the ion core. The easiest way to do this is to numerically look for zero-crossings of the function for a

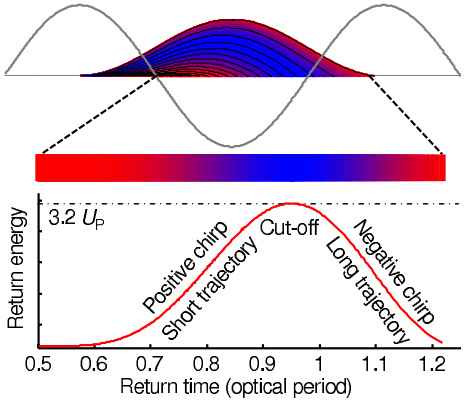


FIG. 4: Illustration of the physics of high-order harmonic generation. The top figure shows classical electron trajectories for different initial phases relative to the IR laser field (black lines). The electron returns to the atom when it crosses again the horizontal dotted line. The color illustrates the variation of the kinetic energy for the different trajectories (blue means the highest energy). The bottom figure shows the energy gained by the electron in the continuum, as a function of the time when the electron returns to the core. This simple calculation shows the existence of short and long trajectories separated by the cut-off (maximum energy), as well as the frequency variation in time of the attosecond burst.

range of tunneling times. Note that it is only necessary to examine tunneling times in the range $0 \leq \omega t_i < \pi$ since the process is periodic with the frequency $2\omega$. We also observe that certain trajectories have multiple return times. In reality, the probability for harmonic emission from electrons that have spent more than one period in the laser field rapidly decreases due to the quantum spreading of the wave packet.

*Return times and energies*

For tunneling times such that the electron may recombine with the ion core, i.e. tunneling times found in the previous section, one can calculate the corresponding return times and return energies. The return times are simply the times $t = t_r$ for which Eq.3 has a zero-crossing and the return energies are the kinetic energies at times $t_r$:

$$E_{kin} = 2U_P(\cos(\omega t_r) - \cos(\omega t_i))^2 \qquad (4)$$

A plot of the return energy as a function of return time should look like to the lower part of Fig. 4. (Knowing the value of $E_0$ allows one to rescale the vertical axis to show harmonic order.) It is possible to verify from the plot that the cut-off energy for harmonic generation is $I_P + 3.2U_P$.

In the plot we also see that the return energy curve has two branches: each harmonic energy can appear as a result of two different trajectories. There is always a short trajectory, for which the return time is less than the return time corresponding to the cutoff - and there is a long trajectory, for later return times. The short and long trajectories are named after the excursion time of the electron in the continuum ($t_r - t_i < 0.65, /T$ for the short trajectories and $t_r - t_i > 0.65, /T$ for the long). From the figure, we observe that the return times for both trajectory classes changes with return energy, implying a streaking in time of the frequency components of the harmonic emission. For the short trajectory class, the frequency of the light burst increases with time, in other words the pulse is positively chirped, and for the long trajectory class the frequency decreases with time, i.e. the light burst is negatively chirped. The two trajectories differ in excursion time, i.e. they have different continuum dynamics, leading to a significant difference in the properties of the emitted light. For example, their divergence is different. This allows us to attenuate the contribution for one trajectory class by simply aperturing the radiation, without affecting the other, more collimated trajectory class.

Hint: It is convenient to express time variables in $\omega t$, and energy in $U_p$; this way one does not need to explicitly state the intensity and frequency of the field.

From this simple, qualitative investigation we can conclude that for each half-cycle of the driving frequency, a broad spectral continuum of light is emitted, corresponding in the temporal domain to a short pulse. As discussed above, in the spectrum we observe discrete peaks at odd harmonic frequencies because the generation process is periodic with a period of $T/2$. In the temporal domain this means that instead of generating a single attosecond pulse, we obtain a train of attosecond pulses.

This classical model can be simplified even further, to allow discussions at a high-school level: in order to avoid calculus, the laser electric field can be approximated by a square function. The students should be explained that in a linearly-polarized light field, atoms may become ionized, and the freed electron (appearing at a time $t_i$ right next to the ionic core with zero initial velocity), driven by the electric field might return to the ionic core. They can find the time interval for $t_i$ during which the return of the electron may occur, and obtain the maximum of the kinetic energy of the returning electron.

A recent experimental study of plateau harmonics, generated in argon and neon, showed that the frequency components of the XUV radiation are not exactly synchronized, and that the XUV pulses consequently exhibit a significant chirp (frequency variation in time) [7, 18]. This intrinsic chirp comes from the fundamental electron dynamics responsible for HHG.

Under most experimental conditions, the short trajectories are favored by phase-matching conditions [19], making it dominate over the long trajectory. With only the short trajectory present, the XUV bursts will have

an almost linear chirp that can be compensated for [7].

The classical approach we have used here is not strictly correct. In a quantum mechanical description [20], the single electron does not follow a single trajectory and instead we have to use a picture where the electron wave packet is distributed over the different trajectories. In order to complete the picture, we also have to include effects of the actual tunneling process. Qualitatively however, the classical results are in good agreement with both more extensive calculations and with experiments.

The spectral range of the harmonic emission as well as the conversion efficiency depends strongly on the gas medium, as well as on the excitation wavelength. The efficiency is highest in the heavy atoms Ar, Xe, Kr, but the highest photon energies are obtained in He and Ne. Similarly, using a longer fundamental wavelength leads to an extended spectral range to the detriment of the conversion efficiency in the plateau region. This can be qualitatively understood with arguments derived from the three-step model: atoms with high ionization potential can be exposed to a high laser intensity before being ionized. The maximum kinetic energy acquired by the electron increases while the probability for recombination and emission of radiation at a particular energy decreases.

## MEASUREMENT TECHNIQUES

The fastest electronic detectors today have a resolution limit of about 1 ps, making them inappropriate to trace processes on the time scale discussed here. The most direct method to characterize the temporal structure of the pulses is to use a non-linear autocorrelation technique exploiting two-XUV-photon ionization. It requires, however, a high XUV intensity, achieved so far only for low-order processes [8]. Cross-correlation techniques where the XUV pulse is probed by the infrared laser field scale linearly with the XUV intensity and can therefore be used over a broader spectral range. The characterization of attosecond pulses in a train is performed using the method called RABITT (reconstruction of attosecond beating by interference of two-photon transitions), based on mixed-color ionization involving one XUV photon and one driver laser photon [6, 7, 21]. It is a simple and versatile spectrally-based method, ideally suited for the characterization of trains of attosecond pulses. Isolated attosecond pulses are characterized by an alternative technique called the attosecond streak camera, which exploits the dependence of the kinetic energy of the XUV-pulse-generated photoelectron on the phase of the laser field at the instant of photoionization [5, 22, 23].

The principle of the RABITT method can be presented using a simple model based on monochromatic harmonic fields. In this model the total temporal intensity is obtained from the coherent sum of monochromatic spectral components, each characterized by an amplitude $A_q$, a frequency $q\omega$ and a phase $\varphi_q$:

$$I(t) = \left| \sum_{q \text{ odd}} A_q e^{i(q\omega t + \varphi_q)} \right|^2 , \tag{5}$$

where $q$ is the harmonic order and $\omega$ the fundamental frequency. A constant spectral phase, such that $\varphi_q$ is independent of $q$, does not affect the pulse shape and thus a useful and commonly used quantity is the phase difference between two consecutive harmonics, which is defined as

$$\Delta\varphi_{q+1} = \varphi_{q+2} - \varphi_q. \tag{6}$$

With this definition, $\Delta\varphi_{q+1}$ represents the average (group) delay between the $q$th and $(q+2)$th harmonics. $\Delta\varphi_{q+1}/2\omega$ is the return time used in the classical model for an electron returning with the kinetic energy $(q+1)\hbar\omega - I_p$ [18]. The shortest possible attosecond pulse duration is obtained when $\Delta\varphi_{q+1}$ is constant, independent of $q$. In this case, all the frequency components of the pulse "arrive" at the same instant in time. Such a pulse is called transform limited. If $\Delta\varphi_{q+1}$ varies with $q$, the different frequency components of the pulse will arrive at different times, leading to a pulse duration exceeding the transform limit. Furthermore, the instantaneous frequency of the electric field of the pulse will vary in time during the attosecond pulse. This variation of the frequency in time is called chirp. If $\Delta\varphi_{q+1}$ increases monotonically with $q$, the instantaneous frequency will increase linearly with time: the pulse exhibits a positive chirp. If instead the phase difference decreases monotonically, the pulse exhibits a negative chirp.

The harmonic amplitudes $A_q$ are easily accessible experimentally from measurements of the harmonic spectrum. The phase differences $\Delta\varphi_{q+1}$ can be obtained using the RABITT technique, described below. When both the amplitudes and phase differences are known, the temporal profile of an average pulse in the pulse train can be calculated using Eq.5.

## RABITT

To measure the phase difference between two consecutive harmonics ($\Delta\varphi$) a cross-correlation technique based on two-photon transition is used (see Fig. 2). Before the laser pulse is focused into the harmonic generator, a small fraction of the beam is split off using a beam splitter (see the section on the experimental setup). This beam, called the probe beam, is propagated through a variable delay stage and recombined with the harmonic

beam immediately after the aluminum filter using a mirror with a drilled hole in the center. It is crucial to have a good spatial and temporal overlap between the harmonic and probe pulses to produce a cross-correlation signal of IR and high-harmonics (sidebands). The aluminum filter cleans the harmonic beam from the fundamental ($\omega_0$) component of the radiation. The recombination mirror also serves as an aperture to filter out harmonics emerging from the long trajectory, showing a larger divergence than harmonics from the short trajectory [24].

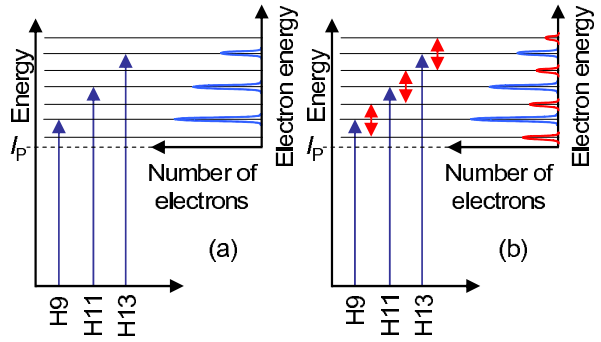


FIG. 5: Sketch of the detected photoelectron spectrum, corresponding to ionization by harmonics 9, 11 and 13, without (a) and with (b) the probe pulse. Ip: ionization potential of the target gas.

To record the photoelectron spectrum, the harmonic beam is re-focused by a platinum toroidal mirror into the sensitive region of a time-of-flight Magnetic Bottle Electron Spectrometer (MBES). The spectrometer is filled to a static pressure of the order of $10^{-5}$ mbar with a detection gas, normally Argon or Neon. Using an arrangement of magnetic fields, the MBES collects ionized photoelectrons emitted within a solid angle of $2\pi$ steradian, directing their trajectories into a flight tube of approximate length 87 cm. At the end of the flight tube, a micro channel plate (MCP) is used for detecting the photoelectrons. Looking temporally at the signal from the MCP, faster photoelectrons resulting from ionization by the higher-order harmonics will arrive first, followed by slower, low-energy photoelectrons resulting from ionization by the low-order harmonics. The actual energy-to-flight-time relationship is determined by the length of the flight tube, as well as by the ionization potential of the detection gas.

$$t_{TOF} = \sqrt{\frac{m_e}{2(\hbar q\omega) - I_p}}\, L_{TOF} \tag{7}$$

Note that the ionization potential of the detection gas sets a limit for the lowest, detectable harmonic order.

In the abscence of the probe beam, the photoelectron spectrum shows peaks at the harmonic frequencies shifted by the ionization potential of the target gas (see Fig. 5a). When the probe pulse overlaps in time and space with the harmonic pulses in the detection gas, two-photon transitions may occur and sidebands appear in the photoelectron spectrum at intermediate energies, due to the absorption of a harmonic photon together with the absorption or emission of an IR photon (see Fig. 5b).

Since the frequency of the IR is exactly half the frequency spacing between consecutive harmonics, there are actually two quantum paths to each sideband (see Fig. 5b). The sideband with energy $(q+1)\,\omega$ has contributions from the absorption of harmonic $q$ plus one IR photon, and from the absorption of harmonic $q+2$ minus one IR photon.

The RABITT technique uses the fact that the two quantum paths to a given sideband interfere, making the sideband intensity dependent not only on the intensity of the harmonic and IR fields, but also on the relative phase between them. When the delay between the harmonics and the probe field is changed, the sideband intensity oscillates. Using a simple perturbative model, it is possible to show that the intensity of sideband $q+1$ is modulated according to:

$$\begin{aligned} I_{q+1}^{(SB)} \propto 1 + \cos\left(2\omega\Delta\tau + \varphi_{q+2} - \varphi_q\right) = \\ = 1 + \cos\ \left(2\omega\Delta\tau + \Delta\varphi_{q+1}\right) \end{aligned} \tag{8}$$

where $\Delta\tau$ is the delay between harmonic and probe pulses [25, 26]. We neglect here for simplicity the small influence of the atomic potential on the measured phases [6, 25]. Fig. 6 shows an experimental RABITT-scan. The photoelectron spectrum is plotted as a function of delay between harmonic and probe pulses, for harmonics 17 to 27 and sidebands 18 to 26. In the practical students carry out an analysis of such a scan to show that the different sidebands does not oscillate in phase, i.e. the peaks of the oscillations do not occur at the same time delay for different sidebands. According to Eq. 8, this means that the phase difference between consecutive harmonics varies with $q$, indicating that the attosecond pulses in the experiment are not transform limited.

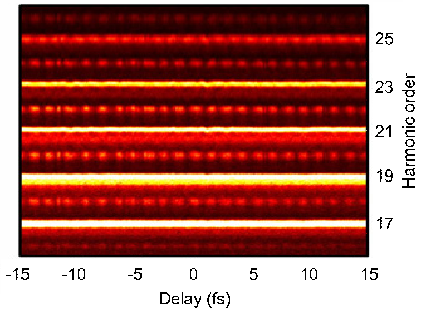


FIG. 6: Experimental recording of a RABITT trace.

### Reconstruction

Using the RABITT-technique, we are able to experimentally determine the phase difference $\Delta\varphi_{q+1}$. As discussed above, together with the measured harmonic amplitudes ($A_q$), this makes it possible to reconstruct the temporal profile of the pulses in the pulse train using Eq.5.

In this reconstruction there are two aspects that have to be addressed. First of all, the reconstruction is based on the assumption, that the harmonics are monochromatic, i.e. infinite in time. Therefore such a reconstruction, only gives access to the average pulse shape of an attosecond pulse in the train. Second, from an ordinary RABITT scan we do not have an absolute reference for $\Delta\varphi_{q+1}$, i.e. we can only measure how the phase difference varies between different sidebands in the scan. Since $\Delta\varphi_{q+1}$ should be interpreted as the group delay between harmonics q and q+2, this simply means that we do not get access to the absolute timing of the attosecond pulses with respect to the generating field [27]. Thus if we only want to determine the average temporal shape of the attosecond pulses, we can simply choose to set the phase difference to zero for one of the sidebands. We do not know either how to choose the absolute value of $\varphi_q$ for the first term in the summation in Eq.5. However, as discussed above, a constant spectral phase does not affect the pulse shape in any way and we may set this to zero as well, without loosing any information necessary for the reconstruction.

### Exercises II

*Pulse reconstruction*

Experimentally one has access to the spectrum, i.e. the amplitudes of the generated harmonics. In the exercise, students can choose a range of harmonics with constant amplitudes, and experiment the influence of different phase behaviors. An average pulse in the pulse train emerging from the superposition of harmonics 13 to 21 or to 29 is reconstructed in Fig. 7.

The effect of the phase behaviour on the pulses is illustrated in Figure 7. When the phase is constant, we talk about a transform limited pulse, which has the shortest duration allowed by the spectral width. A linear phase, corresponding to a constant phase difference ($\alpha$) in $\Delta\varphi(q)$ (i.e. constant delay) contributes to a simple temporal shift of the pulses, but does not change the pulse shape, compared to the transform limited pulse. Whereas a quadratic phase, or a constant increase ($\beta$) in $\Delta\varphi(q)$ corresponds to a chirp and is responsible for the broadening of the pulses. We add here, that the phase difference in HHG varies approximately linearly with harmonic order.

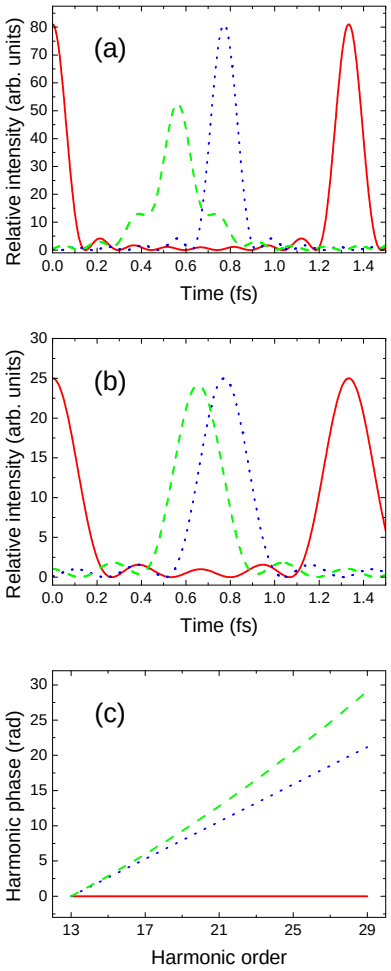


FIG. 7: Intensity vs. time plot of the average pulse in the pulse train, emerging from the superposition of harmonics 13 to 29 (a) and 13 to 21 (b). We show the corresponding phase variation with order (c). Solid line: $\Delta\varphi_{q+1} = 0$ - constant phase. Dotted line: $\Delta\varphi_{q+1} = \alpha$ - linear phase. Dashed line: $\Delta\varphi_{q+1} = \alpha + \beta \times q$ - quadratic phase.

These simple calculations also show that the existence of a chirp reduces the optimum bandwidth over which the shortest pulses can be obtained [18]. Figure 7 (a) and (b) shows the effect of bandwidth on the pulse shapes, we add up nine and five harmonics, respectively. When no chirp is present (solid lines), the attosecond pulses are shorter since the more harmonics are summed up. In the presence of a chirp (dashed lines), adding more harmonics leads to temporal broadening despite of increasing the overall bandwidth.

### Reconstruction of on-target attosecond pulses

After obtaining the temporal overlap between the harmonic and probe pulses in the experimental implementation, we record a RABITT scan similar to that in Fig-

ure 6. The signal produced by the MBES is recorded through an acquisition card of the computer, synchronised to the delay stage motion. The phase difference is measured by looking at the relative positions of the oscillating sideband peaks, and the amplitudes are estimated by integrating the area under each harmonic peak. The harmonic intensities are then corrected for the ionization cross-section of the detection gas. The average attosecond pulse can then be reconstructed based on Equation 5 and connections between the relative phases and the pulse shape can be drawn as explained in Figure 7.

## CONCLUSIONS

In this paper we have described the process of HHG and attosecond pulse production - using an intuitive classical model. At Lund University we have designed a practical for students, containing both an experimental and a theoretical part. This provides the students with a good example of applying concepts from classical physics (and optics) in a newly developing field.

We hope to have explained in a simple, understandable way the basic physics underlying attosecond pulse generation in gases. It is our belief, that by applying their basic knowledge of physical laws to a real-life compound problem, students appreciate more what they have learnt.

This research was supported by the Marie Curie European Program (MRTN-CT-2003-505138), the Knut and Alice Wallenberg Foundation and the Swedish Research Council. KV acknowledges the support of the Magyary Zoltán Postdoctoral Fellowship. PJ is currently with FOM Institute for Atomic and Molecular Physics (AMOLF)

[1] M. Drescher *et al.*, Nature **419**, 803 (2002).
[2] M. Ferray, A. L'Huillier, X. F. Li, *et al.*, J. Phys. B **21**, L31 (1988).
[3] Gy. Farkas and Cs. Toth, Phys. Lett. A **168**, 447 (1992).
[4] S. E. Harris, J. J. Macklin and T. W. Hänsch, Opt. Comm. **100**, 487 (1993).
[5] M. Hentschel *et al.*, Nature **414**, 509 (2001).
[6] P. M. Paul *et al.*, Science **292**, 1689-1692 (2001).
[7] R. López-Martens *et al.*, Phys. Rev. Lett. **94**, 033001 (2005).
[8] P. Tzallas, D. Charalambidis, N. A. Papadogiannis, *et al.*, Nature **426**, 267 (2003).
[9] P.B. Corkum and F. Krausz, Nature Phys. **3**, 381 (2007).
[10] P. Agostini and L.F. DiMauro, Rep. Prog. Phys. **67**, 813 (2004).
[11] G. D. Tsakiris *et al.*, New J. Phys. **8**, 19 (2006).
[12] A. E. Kaplan, Phys. Rev. Lett. **73**, 1243 (1994).
[13] R. W. Boyd, *Nonlinear Optics*, 2nd Edition, Academic Press, 2003.
[14] E. Seres, *et al.*, Phys. Rev. Lett. **92**, 163002 (2004).
[15] K. Schafer, *et al.*, Phys. Rev. Lett. **70**, 1599 (1993).
[16] Corkum, Phys. Rev. Lett. **71**, 1994 (1993).
[17] The reason why it is only the odd and not the even harmonics that are produced, is that there is a phase-shift of $\pi$ between the photons emitted at consecutive events (separated in time by $T/2$).
[18] Y. Mairesse *et al.*, Science **302**, 1540 (2003).
[19] P. Salières, B. Carré, L. Le Déroff, *et al.*, Science **292**, 902 (2001).
[20] M. Lewenstein *et al.*, Phys. Rev. A **52**, 4747 (1995).
[21] H. G. Muller, Appl. Phys. B **74**, S17 (2002).
[22] R. Kienberger, M. Hentschel, M. Uiberacker, *et al.*, Science **297**, 1144 (2002).
[23] R. Kienberger, E. Goulielmakis, M. Uiberacker, *et al.*, Nature **427**, 817 (2004).
[24] M. Bellini *et al.*, Phys. Rev. Lett. **81**, 297 (1998).
[25] Varju *et al.*, Laser Physics, **15**, 888 (2005).
[26] V. Véniard, R. Taïeb, and A. Maquet, Phys. Rev. A **54**, 721 (1996).
[27] L. C. Dinu, H.G. Muller, S. Kazamias, *et al.*, Phys. Rev. Lett. **91**, 063901 (2003).